Scanning tunneling and photoemission spectroscopies at the PTCDA/Au(1 1 1) interface

Nicoleta Nicoara [a,b], Elisa Román [a], José M. Gómez-Rodríguez [b], José A. Martín-Gago [a], Javier Méndez [a,*]

[a] *Instituto de Ciencia de Materiales de Madrid CSIC, Fisica e Ingenieria de Superficies, Campus de Cantoblanco, E-28049 Madrid, Spain*
[b] *Departamento de Física de la Materia Condensada, Universidad Autónoma de Madrid, E-28049 Madrid, Spain*

Abstract

We have studied the electronic properties at the interface of a PTCDA molecular film on Au(1 1 1) by means of scanning tunneling microscopy (STM), scanning tunneling spectroscopy (STS) and angle resolved ultraviolet photoelectron spectroscopy (ARUPS). Measurements were performed for the clean Au(1 1 1) surface as well as for 1 ML and multilayer coverage of PTCDA. STS curves recorded for 1 ML PTCDA film show a feature at the density of states inside the PTCDA gap and a metallic behavior, in contrast to higher coverage, where a semiconductor behavior is observed. By relating this information to the band dispersion of the electronic states close to the Fermi edge, we can assign this electronic feature to the Au(1 1 1) Shockley surface state. By comparison of intramolecularly resolved STM images with first-principles calculations of the free molecule we show that the electronic molecular states at the interface are not altered by the gold surface. All these facts indicate a weak interaction of the PTCDA molecules with the Au surface and we conclude that the observed metallicity of the interface is provided by the gold substrate rather than by the organic layer.
© 2006 Elsevier B.V. All rights reserved.

1. Introduction

In the last years, an intensive research has been focused on organic materials with promising applications in optoelectronic devices [1,2]. These materials incorporate interesting properties such as self-organization, flexibility, new electronic (semiconducting or metallic) and optoelectronic properties. The interface between the organic film and the inorganic material is of special interest, because it influences the structure and morphology of the molecular layers, and hence, also their properties. Therefore, a detailed understanding of the processes taking place at the interface and how they affect the

---

electronic properties of the organic/inorganic system [3] is not only of fundamental importance, but also of technological relevance.

PTCDA (3,4,9,10, perylene tetracarboxylic dianhydride, $C_{24}O_6H_8$) are small conjugated molecules belonging to perylene derivatives, which have been extensively studied along the past years. These molecules are considered as a model system, due to their ability of forming well-ordered layers on a variety of substrates. PTCDA films present semiconducting behavior, strong anisotropy in electronic transport and relevant optical properties [2].

Several studies have focused on the growth mode and structural properties of PTCDA on different metallic substrates: silver [4–8], copper [9,10] and gold [11–16]. Particularly, for PTCDA on Au(111) the structure and morphology of this system have been studied as a function of growth parameters [14]. A layer-by-layer growth has been reported for the first several layers [11], followed by island formation for multilayer coverage [15]. Even in the sub-monolayer regime PTCDA forms large domains with well-ordered molecules. PTCDA molecules typically assemble on most substrates in a herringbone structure, with a rectangular unit cell consisting of two almost coplanar molecules [13,14,16]. For the Au(111) substrate, also a less dense square assembling can be obtained [15], which is not treated in this paper.

Scanning tunneling microscope (STM) has demonstrated its ability for the investigation of ordered organic films grown on different substrates, providing structural and morphological properties. Besides the topographical imaging, information about the surface density of states from the voltage dependence of the current can be obtained from scanning tunneling spectroscopy (STS). The advantage of STS, compared to other spectroscopic techniques, is to locally probe the electronic properties. On the other hand its interpretation is not straightforward due to the convolution with the tip states. In this sense the combination of STS and ultraviolet photoemission spectroscopy (UPS) is a powerful tool to determine electronic properties at the interface.

One aspect treated in this paper is the interaction of the PTCDA molecules with the metallic substrate. In previous works, the interaction of PTCDA molecules with silver surfaces has been described as strong [17], involving an interaction between the π molecular orbitals and the metallic surface. For the Ag(111) substrate, a metallic behavior for the first PTCDA monolayer has been reported [18]. In the case of Au substrates a weaker interaction has been observed [19]. STS measurements for PTCDA grown on gold have been performed [20,21], however, the metallicity of the first monolayer has not been addressed up to now.

Another aspect here mentioned is the influence of the organic molecules on the gold surface state. Tunneling spectroscopic studies have reported on the behavior of the surface states of noble metals [22], and how these surface states are modified by adsorbates [23–27].

In this work we focus on the electronic states close to the Fermi energy of the PTCDA/Au interface by combining STM, STS and angle resolved UPS (ARUPS). Through several experimental observations we assert that there is a weak interaction between the gold substrate and the first organic monolayer, which does not disrupt the Au(111) surface state even though the PTCDA overlayer completely covers the Au surface. We conclude that the metallic behavior of the interface is provided by the gold substrate beneath.

2. Experimental

STM and STS experiments were carried out with a home-built UHV STM [28]. Ultraviolet photoelectron spectroscopy measurements were performed in a separate UHV chamber equipped with a HeI (21.2 eV) radiation source and a hemispheric electron analyzer. The angular aperture of the analyzer is 2°.

Au(111) single crystal sample was cleaned by several sputtering and annealing cycles (sputtering at $\sim 1 \times 10^{-6}$ Ar pressure, annealing at ~ 700 K).

The organic films were deposited under ultrahigh vacuum from home-made sublimation cells. Previous degassing of the PTCDA cell was performed. The deposition rate was about 0.5 ML per minute and was calibrated via scanning tunneling microscopy and previously by a quartz microbalance. Prior to the photoemission experiments, a careful estimation of the PTCDA coverage was performed from XPS measurements (data not shown here).

All the measurements were taken at room temperature. For the STM/STS experiments, tungsten (electrochemically etched) and Pt–Ir (mechanically cut) tips were used. W tips were prepared in situ by thermal annealing and field emission, until stable field emission currents were obtained. For the system investigated here, the most reproducible spec-

troscopic data were obtained with mechanically cut Pt–Ir tips. They were recorded at stabilization bias voltages between −1 and −2.5 V, with voltages referred to the sample. Higher voltages damaged or lifted up the molecules from the surface. Tunneling spectroscopy was performed with set-point currents as low as possible, in order to avoid strong interaction between the tip and the organic layer [29], but high enough to have signal at zero voltage [30]. STS curves were measured by averaging several successive plots obtained on the same position and conditions. All the STM/STS data acquisition and processing were done using the WSxM software [31].

3. Results and discussion

3.1. Scanning tunneling microscopy

Detailed characterizations of the structural properties and the growth mode of PTCDA/Au have been previously reported [11–16]. However, for sub-monolayer coverage several aspects can be discussed from topographic STM images. In Fig. 1 we show a representative STM image of PTCDA molecules deposited at room temperature on a Au(111) substrate for a sub-monolayer coverage. On the left side of the STM image, the clean Au(111) substrate is observed with the characteristic $(22 \times \sqrt{3})$ reconstruction. On the right side, adsorbed PTCDA molecules form an ordered
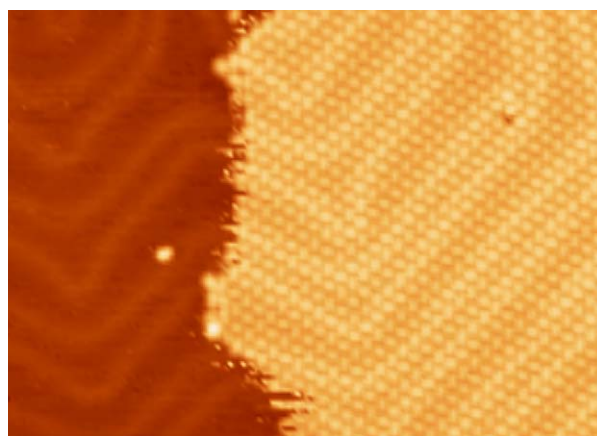
Fig. 1. Constant current STM image of sub-monolayer PTCDA coverage on Au(111). The right side of the image corresponds to a gold terrace covered with 1 ML of PTCDA. The left side corresponds to the clean substrate. The substrate reconstruction is still visible through the organic layer ($57 \, nm \times 40 \, nm$, $V = -2.0 \, V$, $I = 0.16 \, nA$).

domain assembled in the so-called herringbone structure [13,14]. This structure is characteristic of the (102) plane of PTCDA bulk [13]. The noisy appearance in the STM images at the boundary of the PTCDA area is due to a high mobility of PTCDA at room temperature, with molecules diffusing on the surface. Isolated molecules are only observed when they are stacked along the steps or pinned at surface defects.

Another interesting fact is that already in the first monolayer PTCDA molecules adopt a structure similar to the bulk molecular crystal [32]. Furthermore, it can be noticed in Fig. 1 that the Au(111) reconstruction is not lifted up upon PTCDA monolayer adsorption [13,15,16]. The gold reconstruction is still visible underneath the PTCDA molecular layer. All these statements point out towards a weak interaction of the molecules with the gold substrate and that the molecule–molecule interaction dominates over the molecule–substrate interaction [15].

Additional proofs for the weak interaction come from the bias-dependent imaging of PTCDA on gold. In Fig. 2(a) and (c) we show STM images acquired at both polarities on a region covered by 1 ML. In these constant current images we resolve intramolecular features of the PTCDA molecules. The images reveal distinct internal structures for unoccupied molecular states ($V = +1.0 \, V$) and for occupied molecular states ($V = -1.8 \, V$).

For the positive biased sample, where the electrons tunnel into the unoccupied states of the sample, we observe 10 maxima in the STM topographic images (Fig. 2(a)). In the case of a negative bias applied to the sample, which means electrons tunneling from the occupied states, the image reveals eight maxima for each molecule (Fig. 2(c)), and all the molecules present a deeper area parallel to the long axis, which splits the molecules in two parts. Profiles along the molecules have been added for better recognition of the maxima.

In order to gain insight into the meaning of these intramolecular features, we have performed first-principles calculations for the PTCDA free molecule. These calculations were done within density functional theory (DFT) in the local density approximation (LDA) [33], using the SIESTA method [34,35]. Core electrons were replaced by norm-conserving pseudopotentials [36], whereas valence electrons were described using a double-ζ plus polarization (DZP) basis set. A real-space grid with a cutoff of 50 Ry was used. Only the Γ point was used in reciprocal space. The geometries were
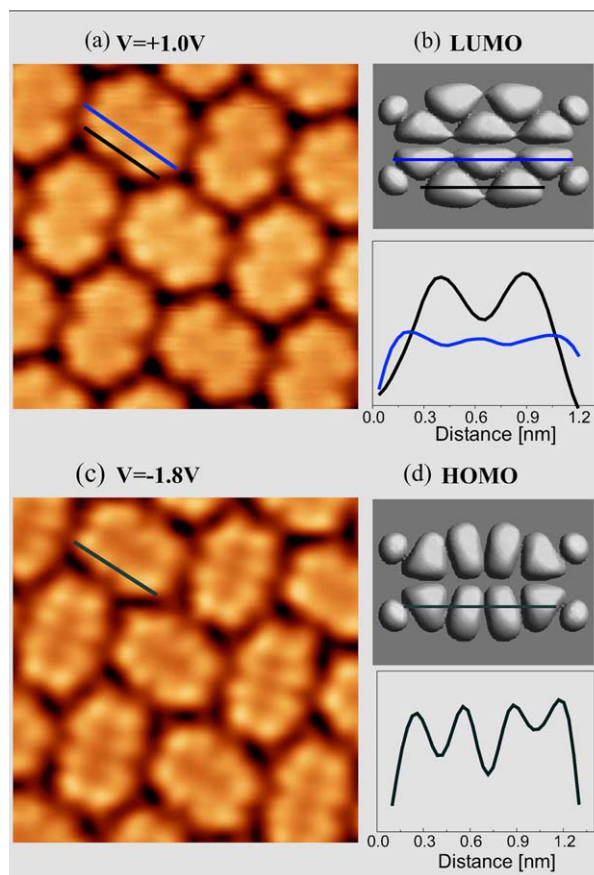
Fig. 2. (a,c) STM images of 1 ML PTCDA on Au(111) at RT obtained at $V = +1.0$ V (unoccupied) and $V = -1.8$ V (occupied), respectively (4.2 nm × 4.2 nm, $I = 0.6$ nA). Notice the similarity between the unoccupied (occupied) states resolved in single molecules and the corresponding calculated LUMO (HOMO) of the free molecule, displayed in (b) and (d), respectively. Profiles along a molecule are shown for better comparison.

relaxed until the maximum residual force was below 0.04 eV/Å.

Fig. 2(b) and (d) present charge density isosurfaces obtained from the DFT calculation and corresponding to the lowest-unoccupied molecular orbital (LUMO) and the highest-occupied molecular orbital (HOMO) of the free molecule [37]. These images are in good agreement with previous calculations by Scholz et al. [38]. The experimental STM image shown in Fig. 2(a), measured at +1.0 V clearly resembles the calculated LUMO of the isolated molecule, while the STM image measured at −1.8 V can be directly related to the calculated HOMO. Although broadening of the orbitals cannot be excluded, the strong similarity between the

calculated orbitals and the STM images (see Fig. 2) suggests that the HOMO and LUMO molecular orbitals, are not significantly modified upon adsorption of PTCDA on gold.

When there is a strong coupling between adsorbate and substrate states, a modification of the electronic structure is expected, and this is generally reflected in the STM image. Thus, for systems with a strong bonding between the organic molecules and the substrate, as PTCDA on Si(100) [39] and on Si(111) [40], high-resolution STM images show that the intramolecular features differ from the HOMO and LUMO of the isolated molecule. Similarly, for PTCDA on silver [41,42] and for PTCDA on graphite [43], where a charge transfer is proposed, shifting of the LUMO towards the Fermi level partially filling this band has been reported [41,43]. In this case, images at both polarities around the Fermi level look like the LUMO. In contrast, for systems where the molecule has a rather weak interaction with the substrate, as reported for pentacene on isolating layers [44] or for the results described in this paper, the intramolecular features resemble the molecular orbitals of the isolated molecule, and this occurs at the corresponding voltages. Again, these findings point out to a rather weak interaction of PTCDA molecules with the gold substrate.

3.2. Scanning tunneling spectroscopy

The main STS measurements were performed for samples with sub-monolayer PTCDA coverage, so that clean gold and PTCDA covered areas could be simultaneously imaged (Fig. 1). Before and after recording spectroscopic data on the adsorbate layer, reference I–V curves were recorded on the clean fcc-gold area. Only when the Au(111) spectrum with the characteristic Shockley-type surface state is achieved, we follow recording current–voltage curves on the PTCDA molecules. With this approach, we ensure a ''good state of the tip'' and therefore, that the additional features which appear in the case of STS on molecules, are indeed related to PTCDA molecular states.

Fig. 3(a) shows tunneling spectroscopy results acquired on the clean Au(111) surface (dashed line) and on the 1 ML PTCDA region (solid line). STS results for 2 ML PTCDA/Au(111) are also included (gray line) for comparison. The spectra are displayed as the differential conductance (dI/dV) vs. V plot. The curve for the clean gold exhibits a characteristic feature, with the onset at ~ -0.4 eV,
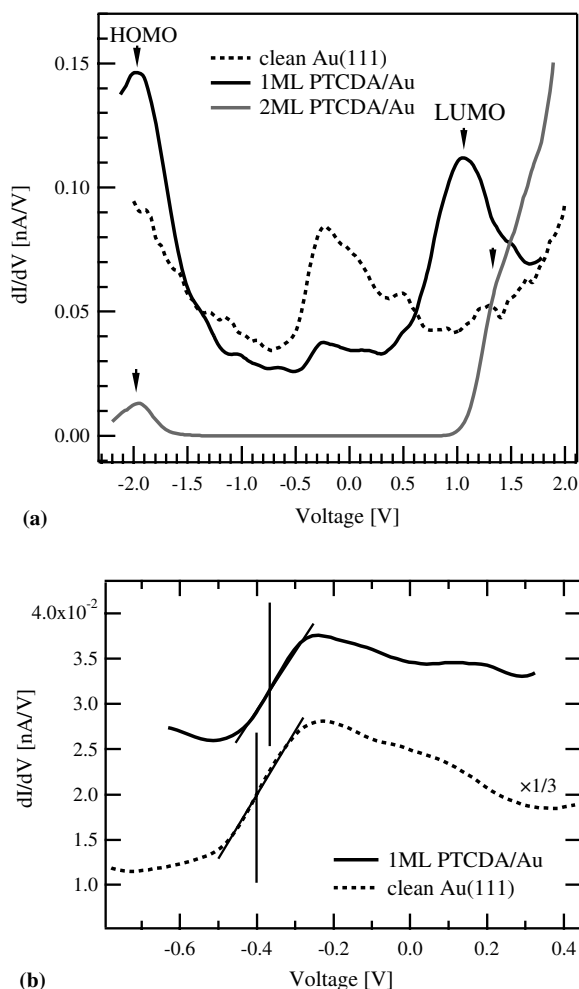
Fig. 3. (a) Tunneling spectroscopy performed at RT on clean Au(111) and on 1 ML PTCDA covered gold. For clean gold (dashed line) the onset of Shockley surface states is identified around −0.4 V. A similar peak and the molecular related features HOMO and LUMO appear in the differential conductance spectra recorded on PTCDA monolayer (solid line). STS for 2 ML PTCDA on gold (gray line) shows semiconducting behaviour characteristic for PTCDA. The plots correspond to the differential conductance that was derived from averaging several *IV* curves and subsequent mathematical differentiation. (b) Detail of the gold surface state region where a shift of ∼40 meV can be observed.

corresponding to the Shockley-type surface state of the Au(111) surface [45,46]. Subsequent spectroscopic curves acquired for 1 ML PTCDA on Au(111) show a metallic behavior characterized by a non-zero density of states at zero voltage. The differential conductance plot for this case (solid line in Fig. 3(a)) shows a peak close to the Fermi level similar to the one observed for the clean substrate though slightly shifted in energy. In the limit

of the room temperature STS experimental resolution,[1] a shift of ∼40 meV toward the Fermi level for the PTCDA monolayer has been reproducibly obtained (Fig. 3(b)). The value of this shift and its direction toward the Fermi level are comparable with STS results reported for rare gases on Au(111) [27], where shifts of 150 meV for Xe and 80 meV for Kr have been obtained. For other adsorbates, the reported energy shift of the bottom of the band is much higher: 300 meV for Pd on Au(111) [25] and 230 meV for NaCl on Cu(111) [26]. These energy shifts can be qualitatively understood as induced by a modification of the image potential and work function of the surface upon coverage [26].

Two additional peaks are observed in the STS results for 1 ML PTCDA (solid line in Fig. 3(a)): one centered around +1.0 V above the Fermi level, and another one around −1.9 V below the Fermi level. These features can be attributed to the lowest-unoccupied (LUMO) and the highest-occupied (HOMO) molecular states of the PTCDA respectively. Tsiper et al. [21] reported these peaks located at +1.3 V and −2.2 V. A possible explanation for this discrepancy could be related to different tip–surface interaction or tunneling distance [29,30].

The STS measurements for 2 ML PTCDA coverage (gray line in Fig. 3(a)) do not show any structure close to the Fermi level, corresponding to the expected semiconductor behavior of the organic layer. In the curve we observe the onset of the LUMO at around +1.0 V, and in the filled states, a peak centered at about −2.0 V attributed to HOMO. The position in energies of both features may slightly shift in the STS spectra depending on the tunneling conditions; the value of the band gap varies between 2.7 and 3.0 eV, when measured from peak-to-peak in the differential conductance (2.4–2.5 eV when measured in the logarithmic representation). For higher PTCDA coverage (3–8 ML), the results are similar to the 2 ML case but the gap increases slightly, approaching a value of 3.3 eV (2.6 eV in the logarithm), in comparison with 2.44–2.55 eV reported for the transport gap of PTCDA [47]. Other authors have reported even lar-

---

[1] The thermal broadening of the STS data measured at room temperature can be estimated as ∼4 kT ≈ 100 meV. This value is compatible with the width of the Au(111) surface-state band onset measured in Fig. 3.

ger gap values [21,48] with a similar dependence with coverage, interpreted as a change in the polarization with the organic layer thickness [21].

The presence of the peak in the STS curves of 1 ML of PTCDA at ~ -0.4 eV (see Fig. 3) is somehow unexpected, since it is known that the organic semiconductor PTCDA has no molecular states in this region, and LUMO and HOMO molecular orbitals are far from the Fermi level. Moreover, this feature being localized close to the Fermi level may confer metallicity to the PTCDA adsorbed layer. Metallicity of the surface overlayer has been reported for PTCDA on the Ag(111) surface [18], where a chemisorption process takes place at the interface. These authors [18] have suggested that the surface state of the Ag(111) could play a significant role in this effect. The question that arises in our case is whether the feature observed in the STS plots belongs to the Au(111) surface states or is rather due to new electronic states formed at the PTCDA/Au interface. The first case suggests a tunneling process of the surface states through the PTCDA layer. On the other hand, the second one points out toward a PTCDA–Au bonding different than a simple Van der Waals interaction that could lead to the formation of states in the overlayer gap. In order to solve this question we have performed ARUPS measurements.

3.3. Angle resolved photoemission

Fig. 4 shows the valence band photoemission spectra recorded at normal emission in the region close to the Fermi level as a function of PTCDA coverage. The peak with a binding energy of 0.4 eV in the upper curve corresponds to the Au(111) Shockley-type surface state [45,46]. In the subsequent spectra we observe that the gold surface state is progressively attenuated as the coverage is increased, being still visible at approximately 1 ML and disappearing at ~ 2 ML coverage (the surface state is still visible at 1.5 ML, as can be observed in Fig. 4). There is no shift, within the experimental resolution, of this electronic state as coverage increases, indicating the absence of important interaction between the layer and the Au surface.

PTCDA related electronic states are not visible in the UPS spectra up to few layers coverage due to the huge contribution and the large mean free path of the valence band gold electrons. No extra states close to the Fermi level can be resolved, neither
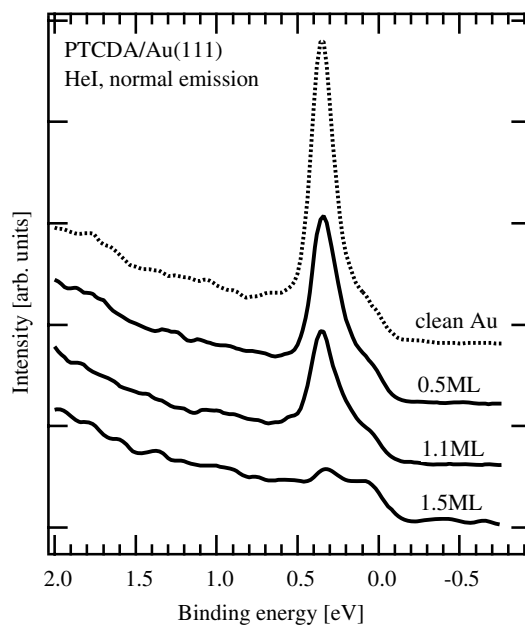
Fig. 4. Normal emission photoemission spectra obtained at room temperature for different coverages of PTCDA on Au(111). The clean Au(111) spectrum shows the Shockley-type surface state at a binding energy of 0.4 eV. For 1.1 ML PTCDA the peak corresponding to the Au(111) surface state is attenuated, but still visible. Binding energies are referred to the Fermi level.

for the PTCDA/Au interface, nor for coverages larger than 1 ML.

Further proofs concerning the behavior and nature of the surface states are provided by angle resolve photoemission (ARUPS) measurements. In Fig. 5 we present the comparison between the photoemission spectra for the clean gold substrate and for a 1 ML PTCDA covered surface as the emission angle is varied close to the surface normal. Both UPS spectra show an identical dispersion, corresponding to the well-known nearly free-electron-like parabolic dispersion of the Shockley-type surface state [46]. It is important to remark that any electronic state related to the single well-ordered PTCDA overlayer should present a band dispersion induced by the lateral periodicity of the layer, which is different from that of Au. Hence, the electronic features should repeat with the surface reciprocal-space lattice i.e., about 0.15 Å^{-1}. This small k-parallel periodicity will be measured in our photoemission experiment as a non-dispersive band. This is not the case of the band shown in Fig. 5, which disperse following the Au(111) periodicity. We can conclude that there are no new electronic features related to the PTCDA–substrate interaction. Hence
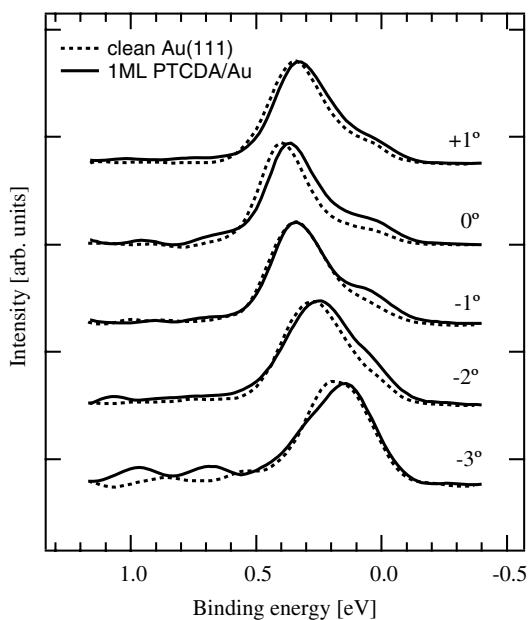
Fig. 5. Angular resolved photoemission spectra for the surface state of clean (dashed line) and 1 ML PTCDA covered Au(111) surface (solid line). Both surfaces display an identical angular dispersion.

the peak observed in the STS curves for the first PTCDA monolayer can be attributed to the Au(111) Shockley surface state. Consequently, the apparent metallicity of the PTCDA monolayer solely arises from the gold substrate beneath; the gold states are detected in the STS experiment via a tunneling process through the PTCDA monolayer.

As mentioned above, adsorption processes typically modify the surface electronic states of the (1 1 1) face of noble metals. By means of photoemission spectroscopy a wide range of effects has been reported depending on the adsorbates and their interaction with the substrate. Chemisorbed atoms often completely quench the surface state [49]. For adsorption (physisorption) of rare gases [27,50], where a weak interaction can be expected, the reported ARUPS energy shift of the bottom of the band is rather small, varying from 150 to 170 meV for Xe, 80 to 100 meV for Kr, and 60 to 87 meV for Ar (Refs. [50,27], respectively). In the case of PTCDA here reported, limited by the experimental resolution of our room temperature photoemission spectroscopy, the ARUPS spectra is compatible with a small energy shift (lower than 100 meV), in agreement with the STS data shown in Fig. 3(b). This places the organic monolayer of PTCDA as a

very weak interacting layer, only comparable to noble gases physisorption.

4. Conclusions

To summarize, we present experimental results obtained from a combination of different spectroscopic methods for the PTCDA/Au(111) interface. The qualitative agreement between experimental data obtained by both techniques, STS and photoemission, gives a clear evidence that the interaction between PTCDA molecules and the Au(111) surface is very weak. The Au(111) Shockley surface state is not disrupted by one single and complete adsorbed layer of PTCDA, but only an small energy shift towards the Fermi level (<100 meV) is observed by both spectroscopies. Therefore, the metallicity observed by STS for the first PTCDA monolayer is provided by the electronic states of the gold substrate tunneling through the organic layer.

References

[1] Hardis Morkoç, Advanced Semiconductor and Organic Techniques, Academic Press, London, 2003.
[2] S.R. Forrest, Chem. Rev. 97 (1997) 1793.
[3] M. Pope, Ch.E. Swenberg, Electronic Processes in Organic Crystals and Polymers, University Press, Oxford, 1999.
[4] C. Siedel, C. Awater, X.D. Liu, L. Ellerbrake, H. Fuchs, Surf. Sci. 371 (1997) 123.
[5] B. Krause, A.C. Dürr, K. Ritley, F. Schreiber, H. Dosch, D. Smilgies, Phys. Rev. B 66 (2002) 235404.
[6] L. Chkoda, M. Schneider, V. Shklover, L. Kilian, M. Sokolowski, C. Heske, E. Umbach, Chem. Phys. Lett. 371 (2003) 548.
[7] L. Kilian, E. Umbach, M. Sokolowski, Surf. Sci. 573 (2004) 359.
[8] D. Braun, A. Schirmeisen, H. Fuchs, Surf. Sci. 75 (2005) 3.
[9] M. Stöhr, M. Gabriel, R. Möller, Surf. Sci. 507–510 (2002) 330.
[10] Th. Wagner, A. Bannani, C. Bobisch, H. Karacuban, M. Stöhr, M. Gabriel, R. Möller, Org. Electron. 5 (2004) 35.

[11] P. Fenter, P.E. Burrows, P. Eisenberger, S.R. Forrest, J. Cryst. Growth 152 (1995) 65.

[12] P. Fenter, P. Eisenberger, P. Burrows, S.R. Forrest, K.S. Liang, Physica B 221 (1996) 145.

[13] T. Schmitz-Hübsch, T. Fritz, R. Sellam, R. Staub, K. Leo, Phys. Rev. B 55 (1997) 7972.

[14] P. Fenter, F. Schreiber, L. Zhou, P. Eisenberger, S.R. Forrest, Phys. Rev. B 56 (1997) 3046.

[15] I. Chizhov, A. Kahn, G. Scoles, J. Cryst. Growth 208 (2000) 449.

[16] S. Mannsfeld, M. Toerker, T. Schmitz-Hübsch, F. Sellam, T. Fritz, K. Leo, Org. Electron. 2 (2001) 121.

[17] V. Shklover, F.S. Tautz, R. Scholz, S. Sloboshanin, M. Sokolowski, J.A. Schaefer, E. Umbach, Surf. Sci. 454–456 (2000) 60.

[18] F.S. Tautz, M. Eremtchenko, J.A. Schaefer, M. Sokolowski, V. Shklover, K. Glockler, E. Umbach, Surf. Sci. 502 (2002) 176.

[19] M. Eremtchenko, D. Bauer, J.A. Schaefer, F.S. Tautz, New J. Phys. 6 (2004) 4.

[20] M. Toerker, T. Fritz, H. Proehl, F. Sellam, K. Leo, Surf. Sci. 491 (2001) 255.

[21] E.V. Tsiper, Z.G. Soos, W. Gao, A. Kahn, Chem. Phys. Lett. 360 (2002) 47.

[22] J. Kliewer, R. Berndt, E.V. Chulkov, V.M. Silkin, P.M. Echenique, S. Crampin, Science 288 (2000) 1399.

[23] J.Y. Park, U.D. Ham, S.-J. Kahng, Y. Kuk, K. Miyake, K. Hata, H. Shigekawa, Phys. Rev. B 62 (2000) R16341.

[24] H. Hövel, B. Grimm, B. Riel, Surf. Sci. 477 (2001) 43.

[25] T. Suzuki, Y. Hasegawa, Z.-Q. Li, K. Ohno, Y. Kawazoe, T. Sakurai, Phys. Rev. B 64 (2001) R081403.

[26] J. Repp, G. Meyer, K.-H. Rieder, Phys. Rev. Lett. 92 (2004) 036803.

[27] T. Andreev, I. Barke, H. Hövel, Phys. Rev. B 70 (2004) 205426.

[28] J.I. Pascual, Ph.D. thesis, Universidad Autónoma de Madrid, 1998; O. Custance, Ph.D. thesis, Universidad Autónoma de Madrid, 2002.

[29] N. Nicoara, O. Custance, D. Granados, J.M. García, J.M. Gómez- Rodríguez, A.M. Baró, J. Méndez, J. Phys.: Condens. Matter 15 (2003) S2619.

[30] R.M. Feenstra, J.A. Stroscio, A.P. Fein, Surf. Sci. 181 (1987) 295.

[31] WSxM-software from http://www.nanotec.es.

[32] S.R. Forrest, Y. Zhang, Phys. Rev. B 49 (1994) 11297.

[33] J.P. Perdew, A. Zunger, Phys. Rev. B 23 (1981) 5048.

[34] P. Ordejón, E. Artacho, J.M. Soler, Phys. Rev. B 53 (1996) R10441.

[35] J.M. Soler, E. Artacho, J. Gale, A. García, J. Junquera, P. Ordejón, D. Sánchez-Portal, J. Phys.: Condens. Matter 14 (2002) 2745.

[36] N. Troullier, J.L. Martins, Phys. Rev. B 43 (1991) 1993.

[37] According to our DFT calculations, the energy difference between the HOMO and the LUMO is 1.6 eV. This value, much lower than the experimental one (it is well known that DFT methods underestimate gap values), is consistent with previous DFT calculations see, e.g., R. Oszwaldowski, H. Vázquez, P. Pou, J. Ortega, R. Pérez, F. Flores, J. Phys.: Condens. Matter 15 (2003) S2665.

[38] R. Scholz, A.Yu. Kobitski, T.U. Kampen, M. Schreiber, D.R.T. Zahn, G. Jungnickel, M. Elstner, M. Sternberg, Th. Frauenheim, Phys. Rev. B 61 (2000) 13659.

[39] T. Soubiron, F. Vaurette, J.P. Nys, B. Grandidier, X. Wallart, D. Stiévenard, Surf. Sci. 581 (2005) 178.

[40] N. Nicoara, O. Paz, J.M. Soler, A.M. Baró, J. Méndez, J.M. Gómez- Rodríguez, in press.

[41] K. Glöckler, C. Seidel, A. Soukopp, M. Sokolowski, E. Umbach, M. Böhringer, R. Berndt, W.-D. Schneider, Surf. Sci. 405 (1998) 1.

[42] A. Hauschild, K. Karki, B.C.C. Cowie, M. Rohlfing, F.S. Tautz, M. Sokolowski, Phys. Rev. Lett. 94 (2005) 036106.

[43] A. Hoshino, S. Isoda, H. Kurata, T. Kobayashi, J. Appl. Phys. 76 (1994) 4113.

[44] J. Repp, G. Meyer, S.M. Stojkovic, A. Gourdon, C. Joachim, Phys. Rev. Lett. 94 (2005) 026803.

[45] S.D. Kevan, R.H. Gaylord, Phys. Rev. B 36 (1987) 5809.

[46] F. Reinert, G. Nicolay, S. Schmidt, D. Ehm, S. Hüfner, Phys. Rev. B 63 (2001) 115415.

[47] T.U. Kampen, G. Gavrila, H. Méndez, D.R.T. Zahn, A.R. Vearey-Roberts, D.A. Evans, J. Wells, I. Mc Govern, W. Braun, J. Phys.: Condens. Matter 15 (2003) S2679.

[48] I.G. Hill, A. Kahn, Z.G. Soos, R.A. Pascal Jr., Chem. Phys. Lett. 327 (2000) 181.

[49] S.A. Lindgren, L. Wallden, Solid State Commun. 28 (1978) 283.

[50] F. Forster, G. Nicolay, F. Reinert, D. Ehm, S. Schmidt, S. Hüfner, Surf. Sci. 532–535 (2003) 160;
F. Forster, S. Hüfner, F. Reinert, J. Phys. Chem. B 108 (2004) 14692.